

# GENERATION OF ATTOSECOND SOFT X-RAY PULSES IN A LONGITUDINAL SPACE CHARGE AMPLIFIER

M. Dohlus, E.A. Schneidmiller and M.V. Yurkov, DESY, Hamburg, Germany

## Abstract

A longitudinal space charge amplifier (LSCA), operating in soft x-ray regime, was recently proposed. Such an amplifier consists of a few amplification cascades (focusing channel and chicane) and a short radiator undulator in the end. Broadband nature of LSCA supports generation of few-cycle pulses as well as wavelength compression. In this paper we consider an application of these properties of LSCA for generation of attosecond x-ray pulses. It is shown that a compact and cheap addition to the soft x-ray free electron laser facility FLASH would allow to generate 60 attosecond (FWHM) long x-ray pulses with the peak power at 100 MW level and a contrast above 98%.

## INTRODUCTION

Longitudinal space charge (LSC) driven microbunching instability [1, 2] in electron linacs with bunch compressors (used as drivers of short wavelength FELs) was a subject of intense theoretical and experimental studies [3, 4, 5, 6, 7, 8, 9, 10]. It was proposed in [11] to use this effect for generation of vacuum ultraviolet (VUV) and x-ray radiation. A concept of a longitudinal space charge amplifier (LSCA) was introduced, scaling relations for an optimized LSCA were obtained, and its possible applications were analyzed. It was pointed out, in particular, that a broadband nature of LSCA supports generation of attosecond pulses. A scheme was suggested that uses the longitudinal space charge amplifier in combination with laser manipulation of the electron beam to produce attosecond soft X-ray pulses. In this paper we describe the operation of the LSCA-based attosecond scheme in details, exemplify it with the parameters of the soft X-ray free electron laser facility FLASH [15, 16] and perform thorough numerical simulations.

## OPERATION OF THE LSCA

The scheme (see Fig. 1) of the longitudinal space charge amplifier (LSCA) [11] is simple both conceptually and technically. An amplification cascade consists of a focusing channel and a dispersive element (usually a chicane) with an optimized momentum compaction  $R_{56}$ . In a channel energy modulations are accumulated, that are proportional to density modulations and space charge impedance. In the chicane these energy modulations are converted into induced density modulations that are much larger than initial ones [1]. In this paper we will consider the case when the amplification starts up from the shot noise. The number of cascades is defined by the condition that the total amplification is sufficient for saturation (density modulation on the order of unity).

The amplified density modulation has a large relative bandwidth, typically in the range 50-100 %. Behind the last cascade a radiator undulator is installed, which produces a powerful radiation with a relatively narrow line (inverse number of periods) within the central cone. This radiation is transversely coherent, and the longitudinal coherence length is given by the product of the number of undulator periods by the radiation wavelength. When LSCA saturates in the last cascade, a typical enhancement of the radiation power over that of spontaneous emission is given by a number of electrons per wavelength.

## DESCRIPTION OF THE SCHEME

First few cascades of LSCA (operate as described above. A broadband density modulation is amplified around the optimal wavelength

$$\lambda_0 \simeq 2\pi\sigma_{\perp}/\gamma, \tag{1}$$

where  $\sigma_{\perp}$  is a transverse size of the beam, and  $\gamma$  is relativistic factor. Length of focusing channel, beta-function, momentum compaction  $R_{56}$  of a chicane are optimized for this wavelength that is defined by the maximum of the LSC impedance. At the same time transverse correlations of the LSC field are on the order of the beam size [4], what guarantees a good transverse coherence.

The last cascade is modified as shown in Fig. 1. A short two-period modulator undulator is installed in front of the last chicane. In this undulator the electron beam is modulated in energy (modulation wavelength is much longer than  $\lambda_0$ ) by a few-cycle powerful laser pulse. A short slice in the electron bunch (between 0 and  $0.3 \mu\text{m}$  in Fig. 2) gets the strongest energy chirp, and is being strongly compressed (by a factor  $C \gg 1$ ) in the following chicane. The  $R_{56}$  of this chicane and the chirp are adjusted such that a required wavelength compression within that slice is achieved, and, at the same time the amplification of the microbunching within the slice through the last chicane is op-

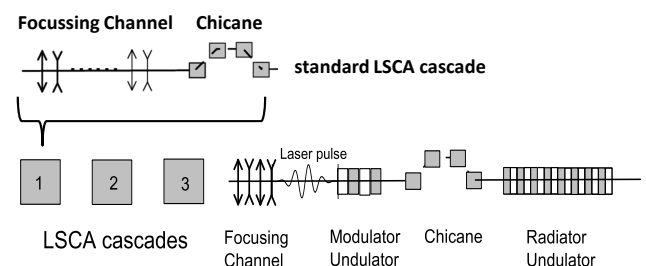


Figure 1: Standard LSCA cascade and LSCA-based attosecond scheme.

timal. Other parts of the electron bunch are either uncompressed or have much weaker compression than the slice with the strongest energy chirp.

The chicane is followed by a short radiator undulator of which resonance wavelength,  $\lambda_0/C$ , corresponds to the (broadband) wavelength spectrum within the strongly compressed slice. Then only this short slice of the electron bunch produces undulator radiation within the central cone (which is selected by a pinhole downstream), while modulation wavelengths in the rest of the electron bunch are much longer than the resonance wavelength of the undulator. In other words, the rest of the electron bunch produces only spontaneous emission within the central cone, and this emission would define the contrast of generated attosecond pulses.

Finally, let us note that broadband nature of LSCA makes wavelength compression especially attractive [11]. Indeed, the compression factor is given by  $C = (1 - hR_{56})^{-1}$ , where  $h$  is the linear energy chirp. For a large  $C$ , the stability of the chirp must satisfy the requirement:  $C\Delta h/h < \Delta k_{max}/k$  with  $\Delta k_{max}$  the maximal bandwidth defined by the modulated bunch and the radiator. This condition might be critical for coherent FEL-type modulations with undulator-radiator, but for LSCA  $\Delta k_{max}/k \simeq 1$ , so that one can go for much stronger compression or loosen the tolerances.

## PARAMETER SET FOR FLASH

We exemplify an operation of the attosecond scheme with beam parameters as they can be reached by the soft x-ray FEL facility FLASH [15, 16]. A 100 pC bunch is compressed to 1 kA and accelerated to 1.2 GeV. A slice energy spread of 150 keV and a normalized emittance of  $0.4 \mu\text{m}$  are expected from beam dynamics simulations in [17] and reduction of compression. For these parameters the optimal wavelength for amplification in LSCA (Eq. 1) is around 40 nm.

The number and parameters of LSCA cascades are chosen with the help of the guidelines in Ref. [11]. Each cascade has a drift of 2.8 m (or two FODO periods) and a total length (with chicane) of 3.5 m. The optimal  $R_{56}$  for a given energy spread and wavelength range is about  $50 \mu\text{m}$ . Three regular cascades and a last special cascade (see Fig. 1) are required so that the total length of the system is about 14 m. A short part of the beam is compressed 8

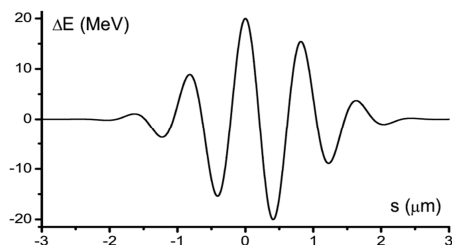


Figure 2: Energy modulation, induced on the beam by a short laser pulse in a two-period undulator.

to 10 times, so that the final wavelength is 4-5 nm. The dispersion parameter  $R_{56}$  of the last chicane is limited by smearing effects due to the uncorrelated energy spread. It has been optimized numerically to  $R_{56} = 7.1 \mu\text{m}$  with an energy modulation as shown in Fig. 2. In order to get the desired energy modulation of 20 MeV amplitude, we use a 800 nm laser pulse with the duration of 5 fs (FWHM) and pulse energy 3 mJ. The laser beam is focused into the modulator undulator, the spot size in the waist is  $w_0 = 300 \mu\text{m}$ . The radiator undulator has 5 periods of  $\lambda_u = 2.5 \text{ cm}$  with a peak field of 0.67 T. We assume that the undulator has a tunable gap which to change wavelength by changing the gap and/or the beam energy.

## NUMERICAL SIMULATIONS

The numerical simulations of the LSCA operation were done as follows. Self-interaction of electrons in the beam by space charge fields in the focussing channels was simulated with 3-D version of the space charge tracking code Astra [18, 19]. All important aspects of the problem like betatron motion of particles in the FODO channel, three-dimensional calculation of the space charge field, start up from shot noise were included in the simulations. To properly treat the start up from noise, we took only a short part of the bunch with the length about  $2 \mu\text{m}$ , and used a real number of particles,  $4 \times 10^7$ , distributing them randomly in 6-D phase space. After the energy change of each particle in a drift was calculated, we simply applied  $R_{56}$  to add the effect of a chicane (later we checked that CSR effects do not play any significant role, see below). In this way the evolution of the particle distribution through a single cascade was simulated. Then the procedure was repeated for the next cascade, etc.

Alternatively, we have developed a simple and fast 1-D code LoSCA (**L**ongitudinal **S**pace **C**harge **A**mplifier). It tracks the particles in the drifts (focussing channel) in presence of an offset independent longitudinal force that is calculated with the LSC wake function, averaged over beam cross-section [20]. The change of particles' distribution through a chicane is again performed by applying  $R_{56}$ . Note that in our particular case the change of particles' longitudinal positions happens only in chicanes. Therefore it is sufficient to calculate energy change of particles due to LSC interaction in only one step per drift (focussing channel). In fact, due to a simple model, used in LoSCA, we were able to relatively quickly calculate the evolution of particles' distribution through LSCA cascades with real number of particles in a bunch (about  $6 \times 10^8$  electrons). To have a representative set of data, we performed several simulation runs with different initial shot noise realizations.

It is interesting to observe that LoSCA gives the same amplification of shot noise modulations as Astra, despite the fact that essentially different models are used in these two codes. We propose the following explanation. Particles in Astra execute betatron oscillations and sample different LSC fields, while in LoSCA there is no transverse motion but the applied LSC wake is averaged over electron beam

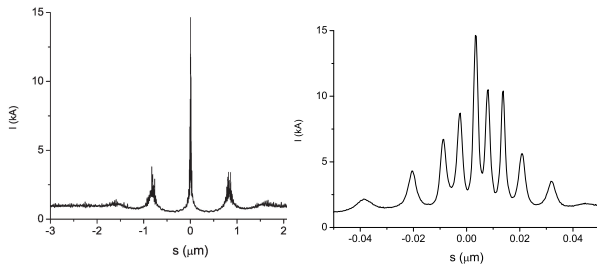


Figure 3: Central part of the electron bunch and a zoomed high-current part after compression in the 4th chicane. The calculations were performed with LoSCA.

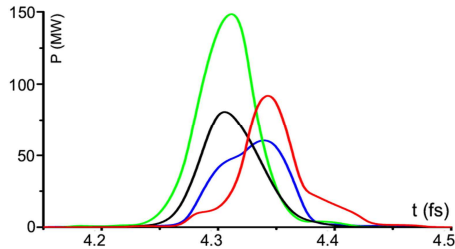


Figure 4: Simulations of the radiation process with the code FAST. Different realizations of attosecond pulses: LSCA was simulated with Astra (black) and LoSCA (red, blue, and green).

cross-section. Therefore both approaches lead to very similar results for the LSCA gain.

In the fourth amplification cascade the beam first moves in the 2.8 m long drift, accumulating energy modulation due to LSC field, and then it is modulated in energy by a short laser pulse. Modulation of the beam by a laser pulse in two-period undulator was simulated in the same way as it was done in [12, 13, 14], namely by a direct integration of equations of motion in the combined field of laser and undulator. The resulting energy modulation is presented in Fig. 2, it was imposed on the phase space distribution of the particles coming from the last drift. Then the effect of the last chicane was simulated by applying  $R_{56} = 7.1 \mu\text{m}$ . A typical current distribution for the beam, simulated with LoSCA, is presented in Fig. 3.

Finally, we did tracking through the chicane, taking into account CSR wake with the help of the projected model [21, 22]. As expected [11], no noticeable effects on longitudinal and transverse dynamics were observed. The reason for this is a practically complete smearing of microstructures inside the chicane due to the coupling of transverse and longitudinal dynamics described by  $R_{51}$  and  $R_{52}$  elements of transfer matrix.

Main simulation results with the code FAST [23] are presented in Fig. 4. Several typical realizations of attosecond pulses are shown, that were obtained from incoming particles' distributions, simulated with Astra (black line) and LoSCA. A typical duration of these pulses is 50-70 attoseconds (FWHM), the peak power is at 100 MW level, and the bandwidth is about 20%. Ensemble-averaged pulse energy is 5 nJ with the pulse-to-pulse rms fluctuations about 35%. One can sometimes observe side peaks (corresponding to those in density modulation in Fig. 3, left plot), but they are

typically below 1% of the power in the main peak. The rest of the bunch radiates only spontaneously (amplified density modulations in the range 20-80 nm could have produced radiation into large angles, well beyond the central cone, but this radiation is totally suppressed due to a finite transverse size of the beam). The half-angle of coherent radiation is about  $50 \mu\text{rad}$ . Selection (with the help of a pinhole) of a cone with half-angle 100-120  $\mu\text{rad}$  would mean that one does not lose any power of attosecond x-ray pulses, while spontaneous radiation background is reduced to the level of 50 pJ for 100 pC bunch. Thus, we can state that a contrast (defined as a ratio of radiation energy of attosecond pulses to the total pulse energy) is high, above 98 %.

## REFERENCES

- [1] E.L. Saldin, E.A. Schneidmiller and M.V. Yurkov, Nucl. Instrum. and Methods **A483**(2002)516
- [2] E.L. Saldin, E.A. Schneidmiller and M.V. Yurkov, Nucl. Instrum. and Methods **A528**(2004)355
- [3] Z. Huang et al., Phys. Rev. ST Accel. Beams **7**(2004)074401
- [4] M. Venturini, Phys. Rev. ST Accel. Beams **11**(2008)034401
- [5] D.F. Ratner, A. Chao, and Z. Huang, Proceedings of the FEL2008 Conference, p. 338, <http://www.jacow.org>
- [6] H. Loos et al., Proceedings of FEL2008 Conference, p. 485, <http://www.jacow.org>
- [7] S. Wesch et al., Proceedings of FEL2009 Conference, p. 619, <http://www.jacow.org>
- [8] A. Lumpkin et al., Phys. Rev. ST Accel. Beams **12**(2009)080702
- [9] M. Clemens et al., DESY Report TESLA-FEL-2009-02, Hamburg, 2009
- [10] Z. Huang et al., Phys. Rev. ST Accel. Beams **13**(2010)020703
- [11] E.A. Schneidmiller and M.V. Yurkov, Phys. Rev. ST Accel. Beams **13**(2010)110701
- [12] E.L. Saldin, E.A. Schneidmiller, M.V. Yurkov, Optics Communications **212**(2002)377.
- [13] E.L. Saldin, E. A. Schneidmiller and M. V. Yurkov, Optics Communications **237**(2004)153-164.
- [14] E.L. Saldin, E.A. Schneidmiller and M.V. Yurkov, Phys. Rev. ST Accel. Beams **9**(2006)050702.
- [15] W. Ackermann et al., Nature Photonics **1**(2007)336
- [16] K. Tiedtke et al., New Journal of Physics **11**(2009)023029
- [17] I. Zagorodnov, "Ultra-short low charge operation at FLASH and the European XFEL", presented at the FEL2010 Conf., Malmö, Sweden
- [18] K. Flöttmann, ASTRA, <http://www.desy.de/mpyflo>, 2000
- [19] G. Pöplau and K. Flöttmann, Proceedings of ICAP2006, Chamonix, France, p. 136, <http://www.jacow.org>
- [20] G. Gelolmi et al., Nucl. Instrum. and Methods **A578**(2007)34
- [21] E.L. Saldin, E.A. Schneidmiller and M.V. Yurkov, Nucl. Instrum. and Methods **A417**(1998)158
- [22] M. Dohlus, DESY report TESLA-FEL-2003-05, Hamburg, 2003
- [23] E.L. Saldin, E.A. Schneidmiller and M.V. Yurkov, Nucl. Instrum. and Methods **A 429**(1999)233